Numerical simulation of inviscid drop oscillations induced by the surface tension

M.N. Shtokolova and V.A. Yakutenok

Tomsk State University

The oscillating process of an inviscid liquid drop induced by the surface tension is considered in two-dimensional formulation. Drop oscillations are numerically investigated in a wide range of initial deformations. The comparisons with the linearized Rayleigh's solution and mass conservation law confirm the reliability of the obtained results. The results obtained with the boundary-element method and the finite-difference realization are compared.

Introduction

Today many works are known devoted to the analysis of behavior of a liquid in the droplet state. However, the drop breakup under surface tension (i.e., self-deformation) has not been simulated until now and the critical values of drop deformation, resulting in the breakup, have not been determined either. Authors of the majority of works restrict themselves to small drop oscillations in two-dimensional,[2] axisymmetric,[1,3] and 3D [Ref. 3] cases because of the effect of numerical instability of applied schemes.

Almost all researchers in this field note, that exact results are possible to be obtained only at small surface deformations. Therefore, authors of each above work resort to various tricks to enhance the algorithm stability, such as redistribution of grid nodes along the free surface at each time step,[2,3] "smoothing" of the potential function along the free surface in a certain number of time steps by means of spline interpolation[2] or Legendre polinomials,[3] the imposing of additional conditions on potential values at free surface points,[2] etc.

The question arises how such interventions into numerical schemes distort the physics of the process. The prevailing "correction" of the algorithm is adjusting the potential value at the free boundary[1] or dynamic boundary condition (Bernoulli integral). This is equivalent to adding a viscosity coefficient in the last equation, thus stabilizing the scheme, but resulting in some oscillation damping. As it was shown in Ref. 2, the adjustment of dynamic boundary conditions can be considered as accounting for the viscosity of the liquid under study; thus, the question about physical correspondence and rightfulness of the above operations is eliminated. Besides, the chosen algorithm for temporal surface evolution significantly affects the calculation stability and results. This question was considered in detail in Ref. 4 for the first time, where it was shown that the use of the third- and fourth-order Runge–

Kutta methods, conventionally stable in their properties, results in weak scheme dissipation and, hence, oscillations of a simulated ideal drop turn out to be weakly damping.

Oscillations of an ideal liquid drop are studied in this work in a wide range of initial deformations. The comparison with the well-known Rayleigh work[5] is carried out. The obtained oscillation periods at various values of initial drop deformation confirm the conclusion[6] about the growing oscillation period with increase of the initial deformation.

Problem statement

Consider the process of nonlinear oscillations of a drop of incompressible ideal liquid under the action of surface tension in the absence of gravity. The oscillating process of the infinite cylinder of the ideal liquid, having the elliptic cross section form with semi-axes a and b and quiescent at a start moment, is simulated in the plane approximation (Fig. 1).
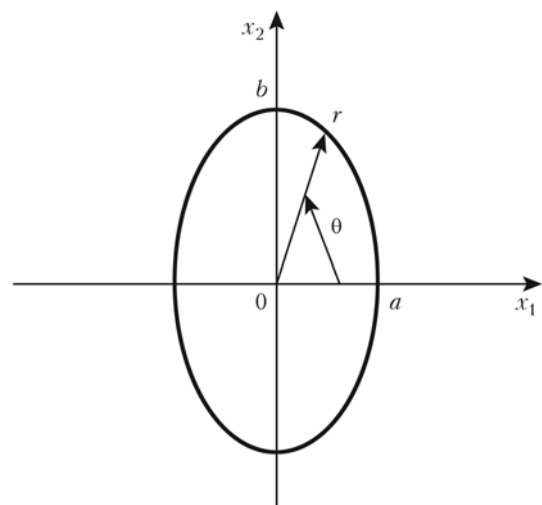
Fig. 1. Oscillations of the infinite volume of ideal liquid in vacuum. Solution region.

Movement of a drop of incompressible inviscid liquid in vacuum or gas of insignificant density can be described with the Laplace equation for the potential φ of the velocity **v**:

$$\nabla^2\varphi = 0, \quad \mathbf{v} = \nabla\varphi. \tag{1}$$

The free surface boundary condition is

$$\frac{d\varphi}{dt} = \frac{v_1^2 + v_2^2}{2} + \frac{\alpha\kappa}{\rho}, \tag{2}$$

where κ is the free surface curvature; ρ is the density; α is the liquid surface stress factor. The free boundary changes in agreement with the kinematic condition, written in the Euler form as

$$\frac{\partial f}{\partial t} + \mathbf{v}\,\mathrm{grad}\,f = 0, \tag{3}$$

where $f(t, \theta)$, is the function describing the drop boundary. The drop is quiescent at a start moment and has the form of oblong ellipse with semi-axes a and b. The ratio of larger and smaller semi-axes $k = b/a$, $k > 1$ is later used as the characteristic of the initial deformation. The initial potential is

$$\varphi = 0. \tag{4}$$

As the characteristic scales, the values are taken

$$R; \ v^* = \left(\frac{\alpha}{\rho R}\right)^{1/2}; \ \varphi^* = \left(\frac{\alpha R}{\rho}\right)^{1/2}; \ T^* = \left(\frac{\rho R^3}{\alpha}\right)^{1/2}, \tag{5}$$

where R is the effective radius of the circle area equal to the area of an ellipse representing the initial free boundary. Thus, in this problem statement, the only parameter determining the character of the stream and characteristics of free surface oscillations is its initial position.

Equation (2) in dimensionless form is

$$\frac{d\varphi}{dt} = \frac{u^2 + v^2}{2} + \kappa. \tag{6}$$

Method of solution

To solve the problem by the boundary-element method (BEM), the passage from the above described differential statement to the boundary integral one is carried out according to the approach given in Ref. 7. To immediately obtain and then solve the singular boundary integral equation, the indirect BEM is used.

Potential and velocity vector's components are calculated at the free boundary. To find its new position, the finite-difference quantization of Eq. (3) is used, where the difference scheme with counter-stream differences is applied[8]:

$$\frac{f_i^{n+1} - f_i^n}{\Delta t} = v_{r_i}^n - v_{\theta_i}^n \frac{\Delta f_i^n}{f_i^n \Delta\theta}, \tag{7}$$

$$\Delta f_i^n = \begin{cases} f_i^n - f_{i-1}^n, & v_{\theta_i}^n > 0, \\ f_{i+1}^n - f_i^n, & v_{\theta_i}^n < 0. \end{cases} \tag{8}$$

Potential at the new free boundary position is defined by means of time and space quantization of the Cauchy–Lagrange integral[6]:

$$\frac{\varphi_i^{n+1} - \varphi_i^n}{\Delta t} = \frac{(v_i^n)^2}{2} + \kappa^{n+1}. \tag{9}$$

Time step Δt is bounded from above by the Courant condition

$$\Delta t \le \Delta S_{\min} / V_{\max}, \tag{10}$$

where $\Delta S_{\min}$ is the minimal element's length; $V_{\max}$ is the maximal velocity attained at some element. As the study has shown, $\Delta t = 0.001$ is quite acceptable at small initial deformations and at the first calculation stage. At large initial deformations (beginning from $k = 1.5$), the time step is chosen automatically by Eq. (10).

To solve the above problem (1), (2), (4), and (6) by the BEM, the coordinate transformation is carried out, at which the domain boundary is transformed to a unit-radius circle:

$$\theta = \theta, \quad \xi = \frac{r}{f(\theta, t)}. \tag{11}$$

Equations (1) and (6) are used in new coordinates. To calculate the potential from the Laplace equation, the Gauss–Seidel scheme is used, and to calculate velocities on the free surface – the following equations:

$$v_r = \frac{\partial\varphi}{\partial r} = \frac{1}{f}\frac{\partial\varphi}{\partial\xi}, \quad v_\theta = \frac{1}{f}\left(\frac{\partial\varphi}{\partial\theta} - \frac{\xi}{f}f'\frac{\partial\varphi}{\partial\xi}\right). \tag{12}$$

To find a new free surface position, the finite-difference quantization of the kinematic condition (3) in form (7) is used with counter-stream difference scheme (8). The potential at the new free boundary position is found according to Eq. (9).

Calculation results

The finite-difference calculations were carried out on the grids with $N_r = 6, 12, 18, 24, 36, 48$ equal partitions along r and $N_\theta = 12, 18, 24, 48$ equal elements toward θ. When potential calculating by the Laplace equation, two schemes were approved:
1) Gauss–Seidel scheme and
2) longitudinal-transversal sweep scheme (LTS).[9]

Both schemes are tested on the problem of potential distribution in an infinitely conductive unit-radius sphere, which has an analytical solution.

Table 1 presents the results of test calculations, in which the rate of iterative process convergence (the number of iterations N) has been estimated on different grids when varying the iteration parameter τ for the longitudinal-transversal sweep scheme (LTS), as well as the rate of convergence of the Gauss–Seidel method on the same grids. The convergence has been estimated to $\varepsilon = 10^{-6}$.

As is seen from the above results, a special choice of the parameter τ allows a high rate of iterative process convergence in LTS to be achieved; however, there are grids on which the iteration process is non-convergent due to lack of diagonal transformation in the matrix, e.g., the grid $N_r = 6$, $N_\theta = 12$ at $\tau = 0.5$. Calculations on finer grids (up to $N_r = 64$, $N_\theta = 64$) have shown the dependence $N(\tau)$ similar to $N_r = 24$, $N_\theta = 36$.

Table 1. Test LTS calculation

Parameter τ	LTS, Number of iterations N, grid $N_r \times N_\theta$						
	6×6	12×6	6×12	12×12	12×24	24×24	24×36
0.0001	5450	5380	5450	5390	5390	10040	10040
0.0005	1260	1250	1260	1250	1250	2350	2350
0.0010	670	670	660	670	670	1250	1250
0.0050	160	160	160	160	160	300	300
0.0100	90	90	90	90	90	160	160
0.0500	50	150	50	150	150	50	50
0.1000	90	280	90	—	—	40	40
Gauss–Seidel scheme	120	270	260	440	1140	1680	2950

The initial problem was solved using both Gauss–Seidel scheme and the LTS algorithm. Oscillation periods and sequences of the free surface shapes, obtained with different schemes, coincide within the range of initial deformations $1.005 \leq k \leq 2.0$. Note that the calculation time of one oscillation period is similar for both schemes, despite the results shown in Table 1. This can be explained by the fact that the number of iterations at each next time step decreases much more rapidly for the Gauss–Seidel method than for the LTS one (Fig. 2).
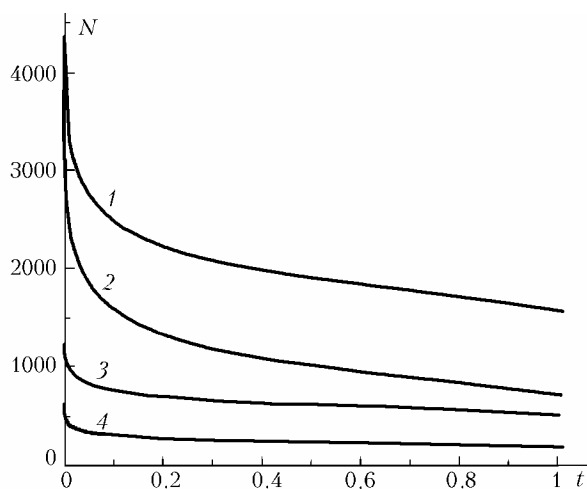
Fig. 2. Numbers of iterations as functions of calculation time: curve *1* and *2* correspond to the Gauss–Seidel scheme, curves *3* and *4* — to the LTS scheme; $\Delta t = 10^{-3}$ (*1* and *3*), $\Delta t = 10^{-4}$ (*2* and *4*); $\varepsilon = 10^{-6}$.

When numerical algorithm implementing, the question about the choice of optimal time step Δt is of importance. The choice criterion is the Courant condition (10). In basic calculations, Δt was equal to 0.001 at the first time step, then Δt was chosen automatically according to Eq. (10).

First, when calculating a new potential value on the free surface by Eq. (9), the curvature κ^{n+1} was calculated at a new free boundary position. In this case, the calculation of oscillations with initial deformation $k > 1.5$ turns out to be impossible because of the zigzag-wise instability at the free boundary. This effect can be avoided if to use the half-sum of curvatures in Eq. (9) $(\kappa^n + \kappa^{n+1})/2$, where κ^{n+1} is the curvature calculated at a new position of the free boundary and κ^n is the curvature from the previous "time layer." It should be noted that this modification of the scheme changes neither oscillation periods no observed free surface shapes.

A series of calculations with different magnitudes of initial axes ratio in the range $1.002 \leq k \leq 2.0$ was carried out by the boundary-element method.[7] In this case, the boundary was partitioned to $N = 96$ constant elements. In calculations with $N > 96$ any differences in period values or free surface shapes were not observed. The evolution of the free surface during oscillating is shown in Fig. 3.

In this work, when simulating drop oscillations with both LTS and BEM, additional "smoothing" procedures for the potential function at the free boundary and for the function describing the boundary were not used (like, for example, in Refs. 1–3), because the imposition of such artificial conditions can distort the simulation results. In this case, we succeeded to simulate the inviscid drop oscillating process in a wide enough range of initial drop deformations (up to $k = 1.5$ for LTS and up to $k = 2.0$ for BEM).

According to classic Rayleigh result,[5] the formula

$$T = 2\pi[n(n - 1)(n + 2)]^{-1/2} \qquad (13)$$

takes place for small oscillations of inviscid liquid in axisymmetric statement. Thus, for $n = 2$ period $T = 2.2214$. It is evident from Fig. 3 that deformation of the free boundary at $t = T/2$, i.e., a half-period of oscillations, corresponds to its initial position. The difference in the initial shape and those at $t = T/2$ is observed at $k = 1.8$. It is seen from Table 2 that T increases with the increase of initial deformation k. At small initial deformations $(1.002 \leq k \leq 1.01)$, the oscillation period of the considered plane approximation differs from the period calculated by Eq. (13) by 14.8%. The area of considered cross section remained invariable to within 0.002% during the oscillating process.

According to the study, beginning from $k = 1.9$, dumb-bells-like free surface shapes are observed during oscillating (see Fig. 3).
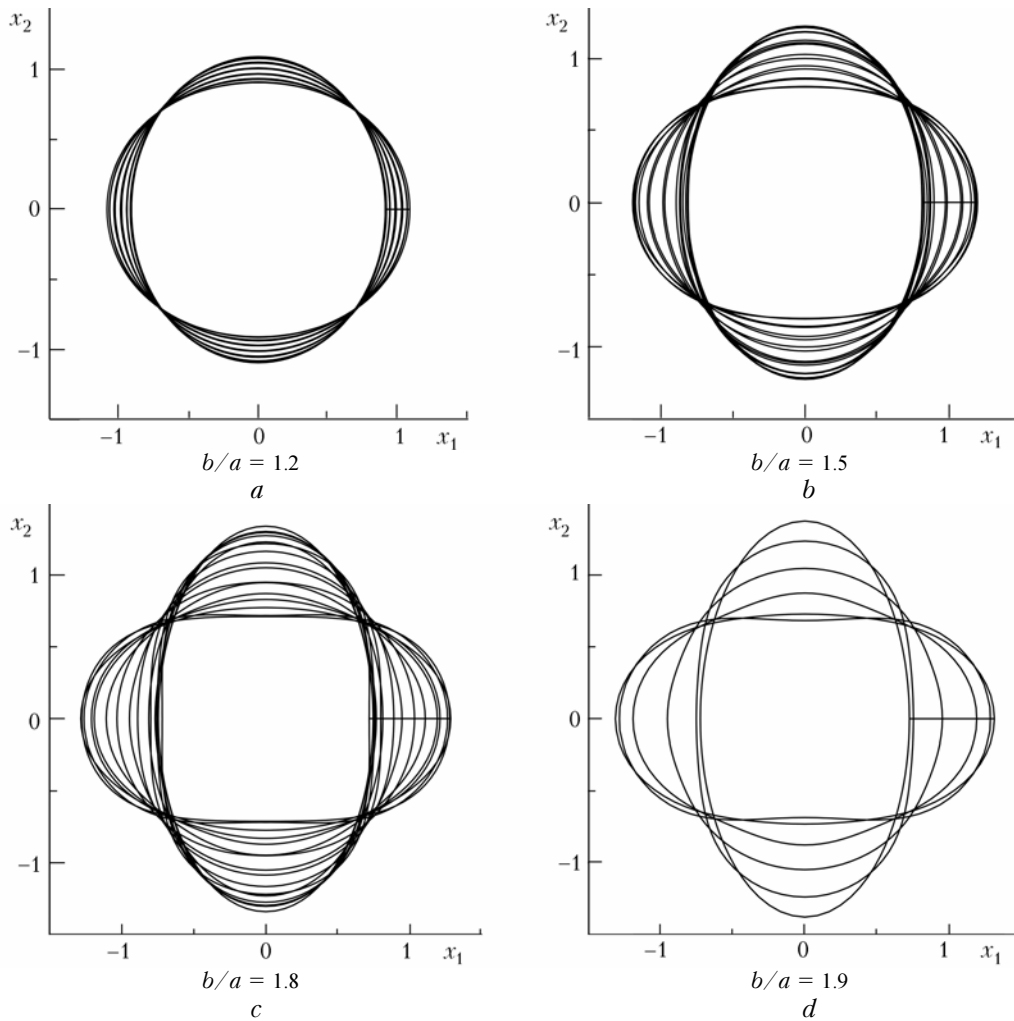
Fig. 3. Free surface shapes, 2D case. Initial deformation $k = 1.2$ (*a*), 1.5 (*b*), 1.8 (*c*), 1.9 (*d*).

Table 2. Results of calculations with boundary-element and Finite-differences (FD) methods

Semi-axes ratio k	Period T	
	BEM	FD
1.01	2.55	2.47
1.10	2.57	2.48
1.20	2.61	2.50
1.50	2.72	2.56
1.70	2.79	2.60
1.80	2.82	2.62

Finally, oscillation periods in a wide range of initial deformations are also obtained from LTS calculations (see Table 2). Free surface shapes, obtained with the LTS, are not given because of their perfect analogy with those obtained earlier with BEM (see Fig. 3). The oscillation periods obtained by both methods confirm the conclusions of Ref. 6, where it has been shown, that the oscillation period of an inviscid drop increases with the oscillation amplitude increase; this is due to initial drop deformation in the case under study.

References

1. T.S. Lundgren and N.N. Mansour, J. Fluid Mech., No. 194, 479–510 (1988).
2. B.M. Rush and A. Nadim, Eng. Anal. Bound. Elements, No. 24, Iss. 1, 43–51 (2000).
3. C. Pozrikidis, Computers & fluids **30**, Iss. 4, 417–444 (2001).
4. G. Colicchio and M. Landrini, J. of Eng. Math. **46**, No. 2, 127–146 (2003).
5. D. Rayleigh, *Sound Theory*. Vol. 2. (Gostekhizdat, Moscow, 1944), 476 pp.
6. J.A. Tsamopoulos and R.A. Brown, J. Fluid Mech. **127**, 519–537 (1983).
7. K. Brebbia, L. Browbel, and J. Teles, *Boundary-Element Methods* [Russian translation] (Mir, Moscow, 1987), 524 pp.
8. P. Rouch, *Computational Hydrodynamics* (Mir, Moscow, 1980), 616 pp.
9. N.N. Yanenko, *Fractional Step Methods for Solving Multidimensional Problems of Mathematical Physics* (Nauka, Novosibirsk, 1967), 197 pp.